Fracture 1977, Volume 3, ICF4, Waterloo, Canada, June 19 - 24, 1977

THE ROLE OF ACOUSTIC EMISSION IN FRACTURE TOUGHNESS TESTING[1]

M. A. Hamstad* and A. K. Mukherjee**

INTRODUCTION

Acoustic emission response to microstructural changes can be very useful [1] in fracture toughness investigations. Several authors [2, 3, 4] have suggested that voids which nucleate by the cracking of nonmetallic particles grow and coalesce during deformation leading to final rupture. Joining of the large voids initiated at the large inclusions often occurs through the matrix by a mechanism of void sheet formation. This formation seems to develop through the formation of voids at submicron size precipitate particles. Fracture toughness might be measured with acoustic emission (AE) response, because both fracture toughness and AE depend on the size and distribution of the phases in the microstructure.

Quite often critical materials components for structural applications are required to meet certain minimum fracture toughness specifications. The cost of inspection, in order to ascertain that such fracture toughness criterion can be met, can be a significant part of the total materials cost. Thus it is often helpful to develop less costly inspection techniques.

The experimental results reported here are a study of the possible application of acoustic emission (AE) as an inspection technique to determine whether or not plates of 2124-T851 aluminum meet certain minimum fracture toughness specifications. The AE generated during both tensile and compression tests of unflawed samples taken from the principal orientations in three plates of 2124-T851 with differing fracture toughness was studied.

EXPERIMENTAL

Specimens were taken from three 2124-T851 plate sections supplied to us by Kaiser Center for Technology. The fracture toughness of the three plates had been previously determined to be 25.1, 28.7 and 34.6 $MPa \cdot m^{1/2}$. These plates were manufactured to give a wide variation in fracture toughness and they all met the nominal chemical specifications. The orientations and locations from which the specimens were taken are illustrated in Figure 1.

The acoustic emission system consisted of: (a) a piezoelectric resonant-type transducer that was coupled to the gauge section of the specimen by a viscous resin; (b) a preamplifier that gave a nominal electronic gain of 60 dB; (c) an amplifier that gave an additional 40 dB electronic gain (the amplifier bandpass was set for 100 to 300 kHz); (d) an oscilloscope that monitored the AE signal; and (e) the AE data presentation system,

* Department of Mechanical Engineering, Lawrence Livermore Laboratory, Livermore, California 94550, U. S. A.
** Department of Mechanical Engineering, University of California, Davis, California 95616, U. S. A.

which primarily consisted of the dc output from a root-mean-square (rms) voltmeter or a true-mean-square (tms) voltmeter. The details of experimental conditions to minimize extraneous acoustic noise from grip or machine fixtures etc., have been reported previously [1]. A clip gauge attached to the specimen gauge section indicated the strain and strain rate. The specimen load was determined with the weighing table on a standard test machine.

RESULTS AND DISCUSSION

Both tension and compression tests were completed for the two principal orientations in the rolling plane (stress axis parallel to and perpendicular to the rolling direction). Figures 2 and 3 show the typical rms of the AE and the stress both as a function of total strain for a tension and a compression test, respectively.

There are several general observations that can be made from the test results: (a) the stress vs. strain curves ordered such that the flow stress was always lowest for the high fracture toughness plate; (b) the AE signal generated in the tensile tests was observed to be quasicontinuous while that for the compression tests was relatively continuous; (c) the rms of the AE exhibited a single peak in the tension tests at approximately 1.5 to 2% of total strain and two peaks in the compression tests. The first peak in compression tests occurred at the point of first macroscopic plastic deformation and the second peak at approximately 2.2 to 3.5% total strain; (d) the comparative peak energy release rates (as sensed by the AE transducer) in the tensile tests was at least two orders of magnitude greater than that for compression tests at the same orientation for the same volume of material undergoing deformation at the same plastic strain rate. This characteristic was previously observed in 7075 aluminum [1]; and (e) the ordering of the peak of AE fell into either of two categories according to plate fracture toughness. Category I from highest peak AE to lowest peak AE followed the sequence of low-to-medium-to-high fracture toughness. Category II from highest peak AE to lowest peak AE followed the sequence of medium-to-high-to-low fracture toughness. Orientations in Category I were longitudinal compression, long transverse tension and short transverse tension. Orientations in Category II were longitudinal tension, long transverse compression and short transverse compression.

Several authors [2, 3, 4] have pointed out that the fracture process and properties in such aluminum alloys are primarily determined by second phase particles and precipitates. The important factors are the sizes and distributions of these particles as well as their resistance to decohesion from the matrix and to cleavage failure. These second phase particles have been divided into three groups: (a) coarse Fe, Si, Mn and Cu rich inclusions approximately 1 to 20 μm in size, which form during casting often at grain boundaries; (b) intermediate Cr, Mn and Zr rich particles, approximately 0.05 to 0.5 μm in size, formed during ingot homogenization, hot-rolling and solution treatment; (c) small precipitates, approximately 0.01 to 0.1 μm in size, formed during the aging heat treatment.

The fracture surfaces of these aluminum alloys have two populations of dimples which participate in the dimpled rupture fracture process. Nucleation of voids by cleavage failure of the coarse brittle inclusions occurs first resulting in the more widely spaced dimple population, second void growth within the matrix as a result of further deformation and third,

a linking up of these voids with participation by the intermediate particles (possibly by decohesion) resulting in the smaller more closely spaced dimple population.

The fracture behaviour of these three plates of 2124-T851 follows the above general model quite closely. Electron microprobe studies of polished samples showed the coarse particles to be elongated in the rolling direction as well as to be high in Fe and to have significant Mn content. Scanning electron microscope studies of the longitudinal tensile fracture surfaces indicated much more brittle type failure for the low fracture toughness specimens and a more ductile failure mode for the high fracture toughness specimens.

The primary source of the AE generated during the unflawed tension and compression tests is believed to be the fracture of the coarse particles. It is unlikely that dislocation motion directly gives rise to AE in this case, although it may help in fracturing the particles by a pile-up process. This hypothesis is supported by the difference in the levels of energy rate out of the AE transducer for tension and compression tests. If one corrects the rms values according to the half-power dependence on plastic strain rate and volume of the specimen undergoing deformation [5], then the energy rate as sensed by the transducer for a tension test is some two orders of magnitude greater than that generated during a compression test of a specimen taken from the same orientation. This result implies that dislocation types of mechanisms are not the AE source event, i.e., the resolved shear stresses for the glide dislocations would not be much different when the externally applied normal stress is tensile or compressive. We have noted [6] similar results in 7075 aluminum plate with brittle chromium-rich inclusion particles. The results of Van Stone et al [4] and Graham [7] also suggest that the cleavage failure of the coarse particles is the primary source of burst-type AE in unflawed tensile specimens of aluminum alloys.

The above discussion suggests that the AE peak during a Category I test correlates (see Figure 4) with the fracture toughness because that peak level is determined by the size and number of voids generated by the cleavage failure of the coarse particles which have been shown to largely determine plate fracture toughness. For plates whose fracture toughness differed only by a few percent, AE which was representative of the other steps in the fracture process (such as void growth in the matrix and decohesion and/or fracture of the intermediate size particles) would probably also have to be taken into consideration in order to correctly sort out the plate fracture toughness.

The separation of the tensile and compression tests into two categories with respect to fracture toughness ordering seems surprising. Particularly the fact that if tension or compression in one orientation is in Category I, then the *opposite* loading in the same direction is in Category II. We are at present developing a model that assumes that the coarse inclusion particles in the 2124 plates are all axisymmetrical ellipsoids with the major axis of symmetry aligned with the rolling direction. Then on the basis of crack surface area created there are two distinctly different types of particle crack planes possible. The plane with the largest surface area is oriented so that the plane is parallel to the rolling direction (i.e., the major axis) and the plane with the least surface area which is perpendicular to the rolling direction. We propose that loads and orientations in Category I cause the coarse particles to fail such that the crack plane is parallel to the longitudinal direction and that loads in Category II

cause the coarse particles to fail such that the crack plane is perpendicular to the longitudinal direction.

Preliminary investigation provides a qualitative explanation as to why the amplitude of AE is decreased in compression. In the tensile loading case when an inclusion fails the strain energy associated with the primary loading stresses is released. While for compressive loading the tensile strain energy associated with the Poisson induced tensile stresses is released when the inclusion fails. This is part of an ongoing research program to correlate AE with fracture toughness. More detailed microstructural investigation currently underway is expected to shed more light on the experimental observation reported in this paper.

ACKNOWLEDGEMENTS

We thank R. G. Patterson for the mechanical testing, R. Bianchetti and R. Bunch for microstructural analysis and J. Bailey at the Kaiser Center for Technology for the special 2124-T851 plates. Work was partially performed under the auspices of the U. S. Energy Research and Development Administration, Contract No. W-7405-Eng-48.

REFERENCES

1. HAMSTAD, M. A. and MUKHERJEE, A. K., "A Comparison of the Acoustic Emission Generated by Tensile and Compression Testing of 7075 Aluminum", UCRL-77502, November, 1975, Lawrence Livermore Laboratory, Livermore, California, 94550.
2. HAHN, G. T. and ROSENFIELD, A. R., Met. Trans., 6A, 1975, 653.
3. VAN STONE, R. H. and PSIODA, J. A., Met. Trans., 6A, 1975, 668.
4. VAN STONE, R. H., MERCHANT, R. H. and LOW, J. R., Jr., ASTM STP 556, Amer. Soc. Testing Materials, 1974, 93.
5. HAMSTAD, M. A., "On Energy Measurement of Continuous Acoustic Emission", UCRL-76286, December, 1974, Lawrence Livermore Laboratory, Livermore, California, 94550.
6. BIANCHETTI, R., HAMSTAD, M. A. and MUKHERJEE, A. K., "Origin of Burst Type Acoustic Emission in Unflawed 7075-T6 Aluminum", to be published in the Journal of Testing and Evaluation.
7. GRAHAM, L., "Sources of Acoustic Emission in Aluminum Alloys", Proceedings of ARPA/AFML Review of Quantitative NDE, July 15 - 17, 1975, Science Center, Rockwell International, Thousand Oaks, California, 631.

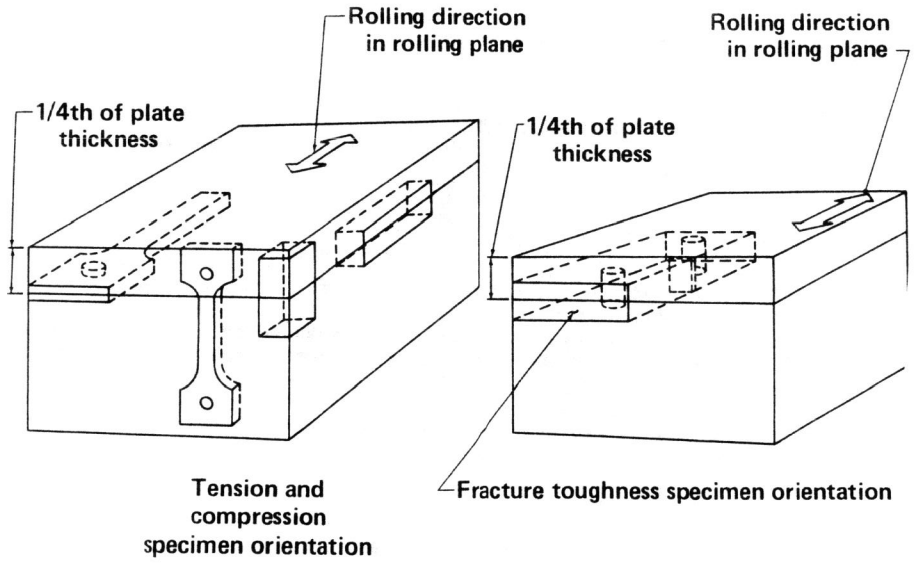

Figure 1 Orientation of Specimens

(a) Tension and Compression Specimens
(b) Fracture Toughness Specimens

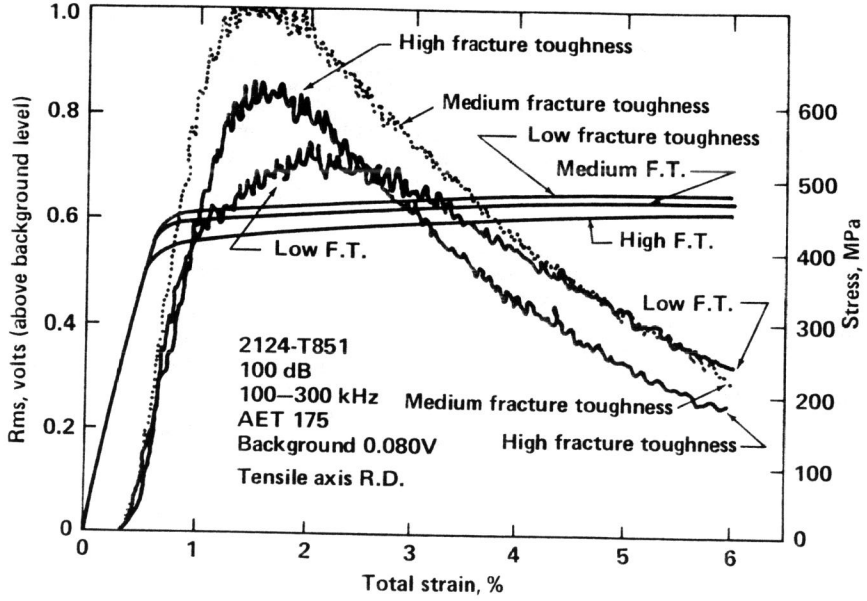

Figure 2 Stress and rms AE versus Total Strain, 2124-T851 Specimens with Loading Axis in Rolling Direction, Tension Test

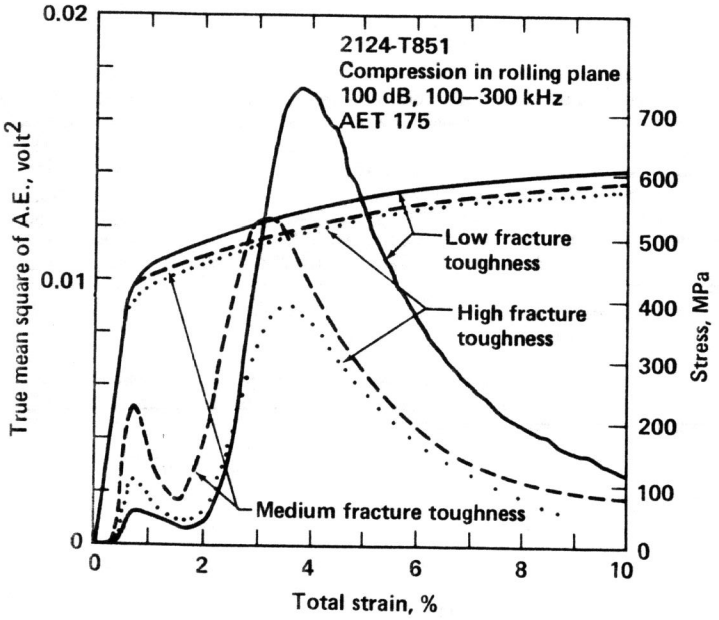

Figure 3 Stress and rms AE versus Total Strain, 2124-T851 Specimens with Loading Axis in Rolling Direction, Compression Test

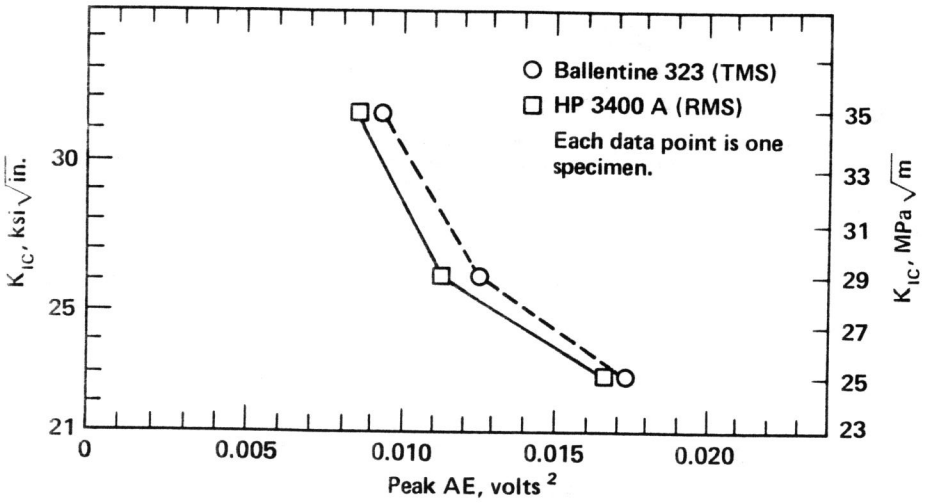

Figure 4 K_{IC} versus Peak AE in $(volts)^2$ for the Three Plates of 2124-T851